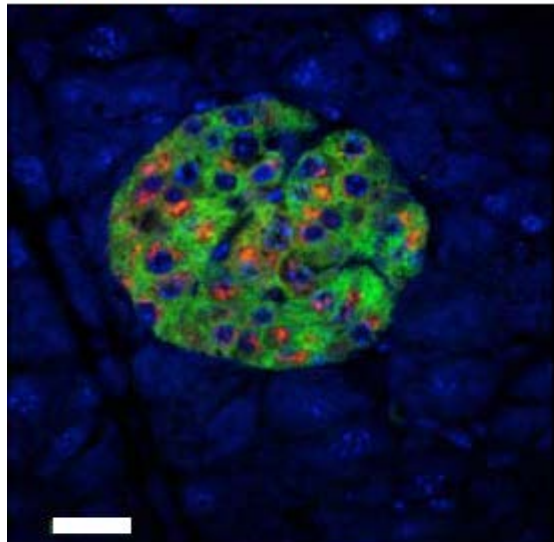


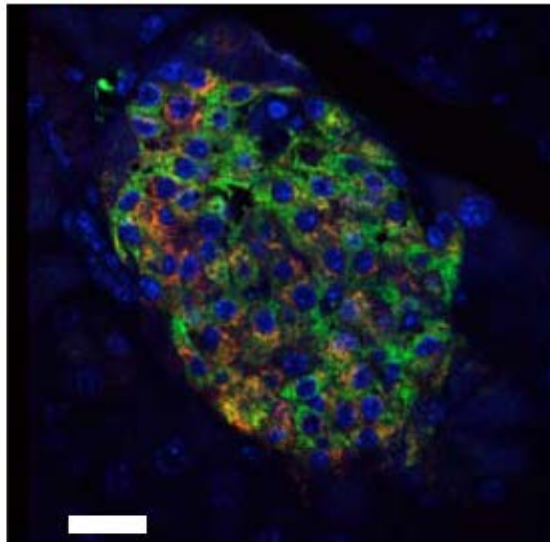
SUPPLEMENTARY DATA

Supplementary Figure S1. Distinct compartmentalization of proinsulin in obese *db/db* mouse islet β -cells. Pancreata from 16-weeks-old $6J^{+/+}$, $6J^{db/db}$, $KS^{+/+}$ and $KS^{db/db}$ mice were harvested, fixed with paraformaldehyde, embedded in paraffin and analyzed by immunofluorescence. Example islet images are shown for insulin (green), proinsulin (red) and DAPI nuclei (blue); bar = 20 μ m.

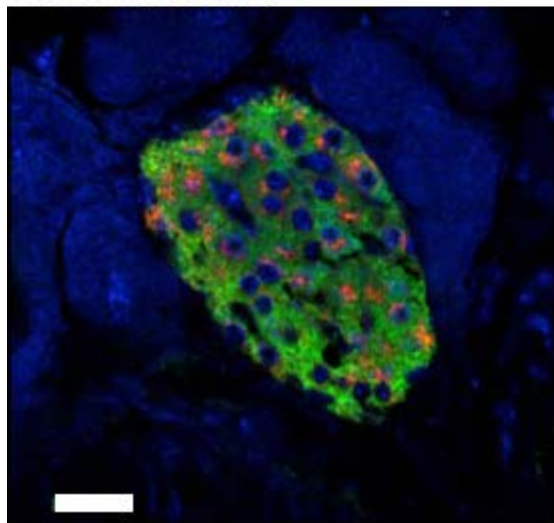
C57BL/6J Control



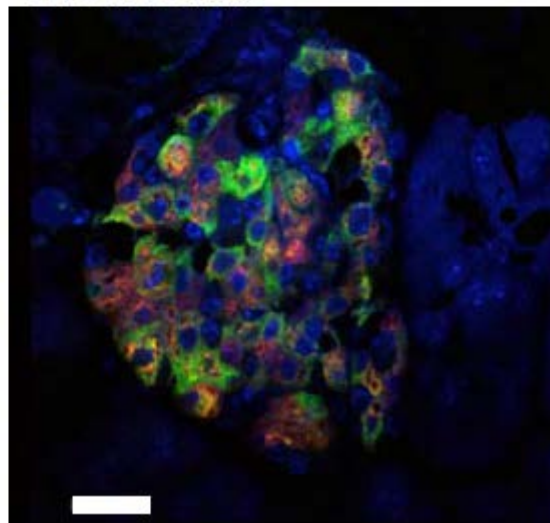
C57BL/6J *db/db*



C57BLKS/J Control



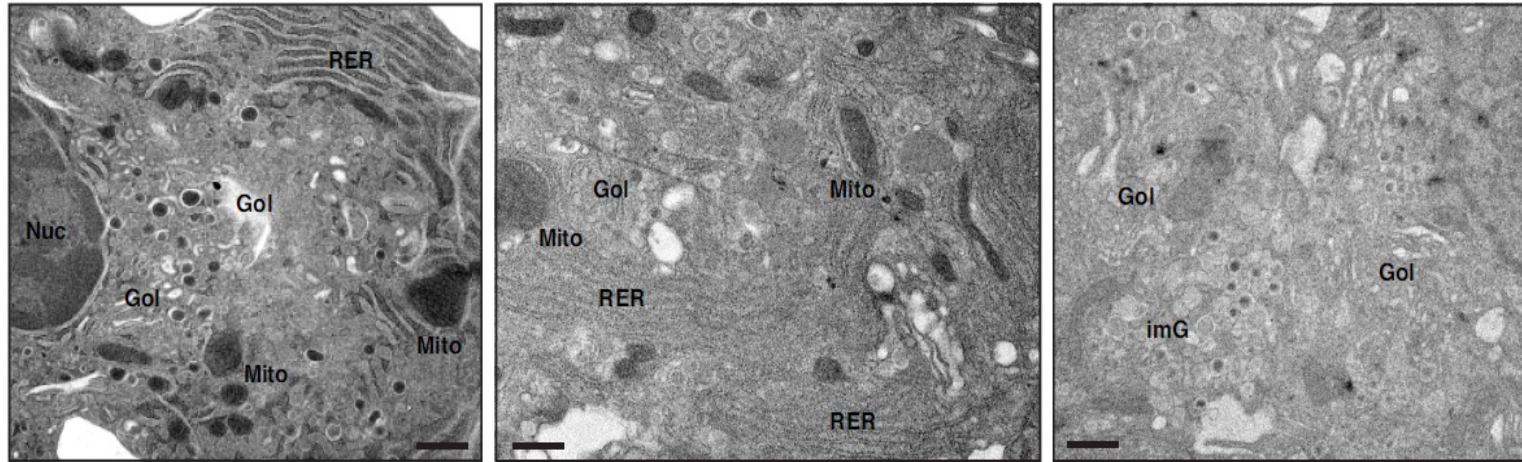
C57BLKS/J *db/db*



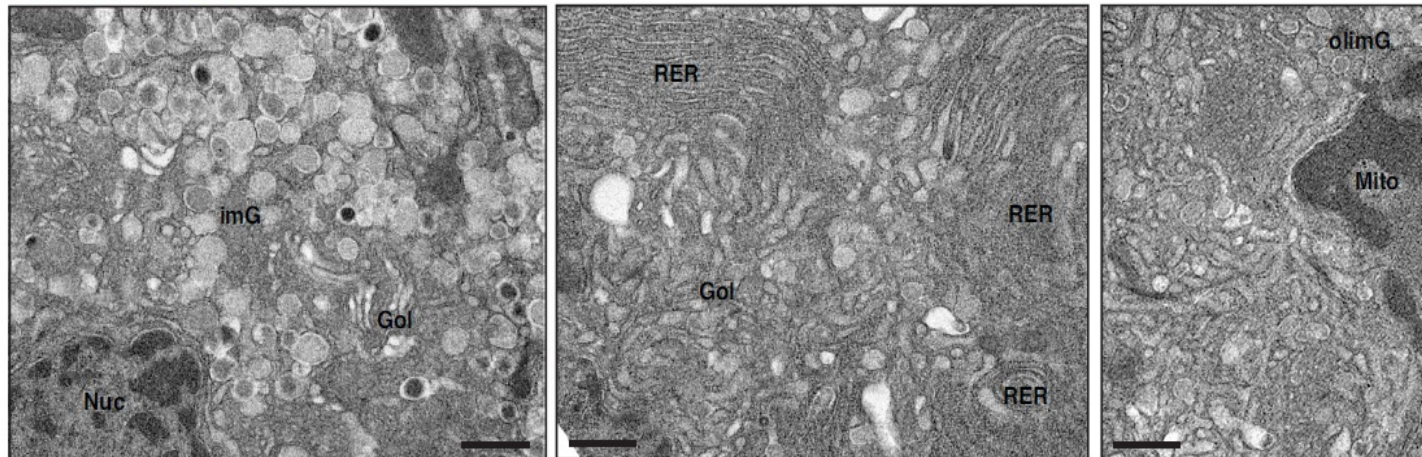
SUPPLEMENTARY DATA

Supplementary Figure S2. Conventional EM analysis of *db/db* mouse islets. Example high-pressure fixed-frozen electron microscopy images of β -cells from freshly isolated *db/db* mouse islets are shown. Expansion of the rough endoplasmic reticulum (RER) and Golgi apparatus (G), decreased number of mature β -granules, and increased number of immature β -granules (IG) are observed.

C57BL/6J db/db

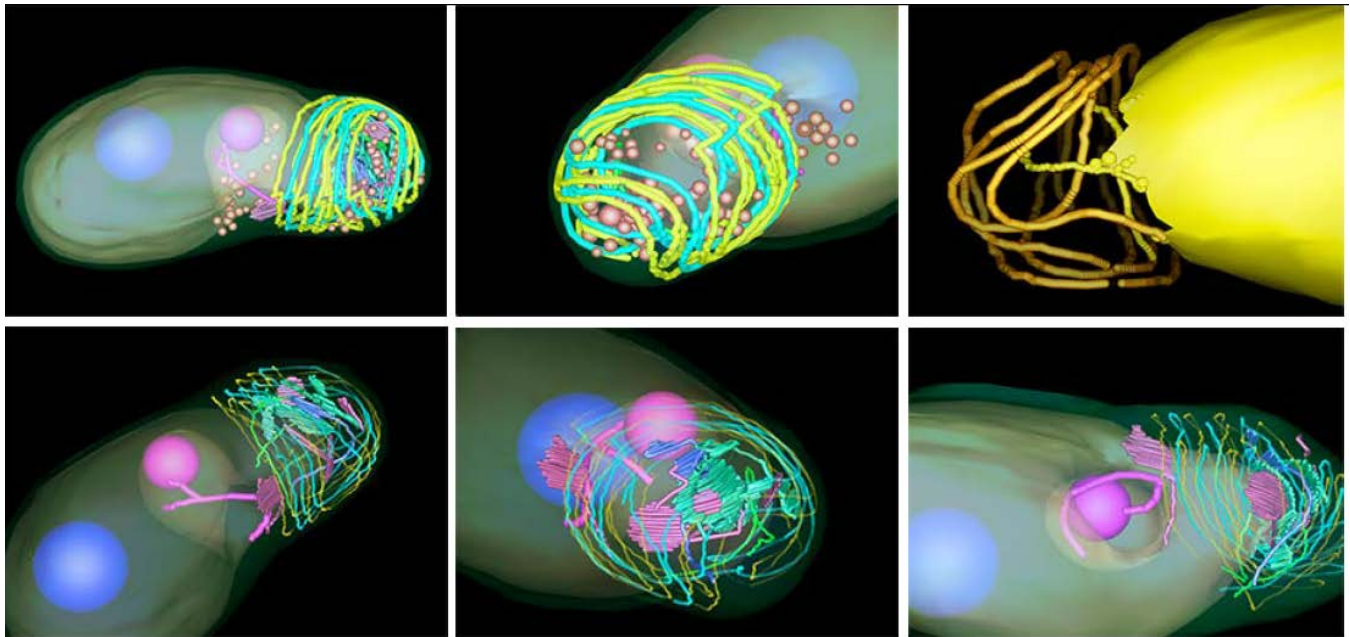


C57BLKS/J db/db



SUPPLEMENTARY DATA

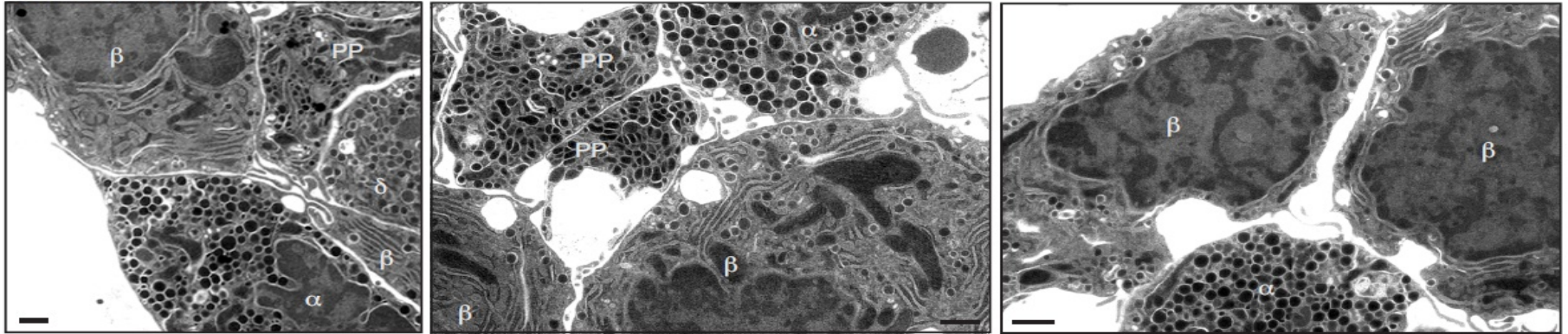
Supplementary Video S1 and Figure S3. EM tomography analysis of a Multivesicular Body (MVB) from a 6J^{db/db} mouse islet β -cell. MVBs were much more frequent in *db/db* mouse islet β -cells than in control islet β -cells, although still too few to quantify. EM tomography and subsequent 3D reconstruction was performed as described in the Methods (Marsh et al., 2007). The Movie S1 shows the compiled stacked images from the EM tomogram melding into a 3D reconstruction of the MVB where each individual membrane bilayer of the MVB is labeled in yellow, pink and blue. A β -granule inside the MVB is shown in purple. Figure S2 compiles various views of the 3D reconstruction of the MVB.



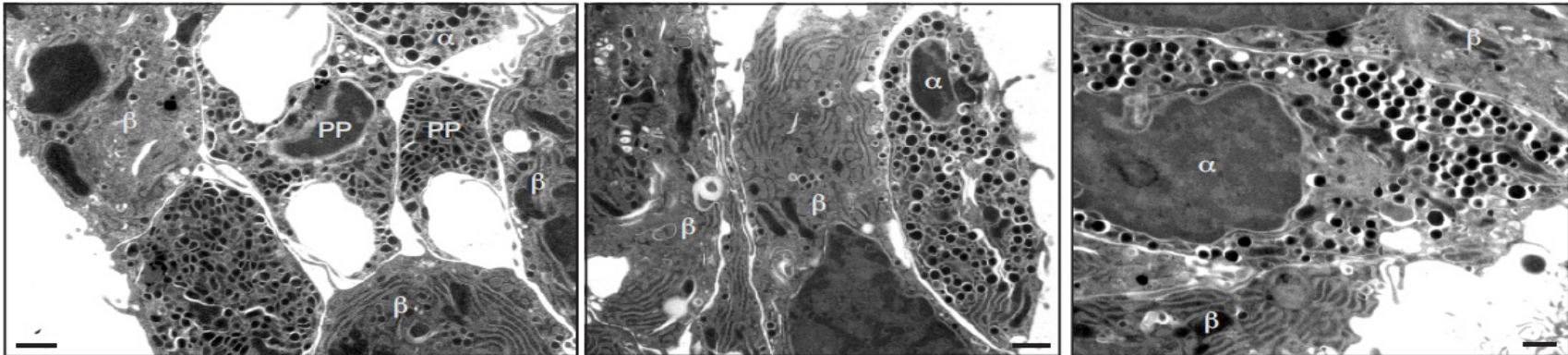
SUPPLEMENTARY DATA

Supplementary Figure S4. Conventional electron microscopy analysis of *db/db* mouse islets. High-pressure fix-freezing electron microscopy images from freshly isolated *db/db* mouse islets showing degranulated β -cells, but normal morphology of α -, δ - and PP-cells in the same *db/db* islets.

C57BL/6J *db/db*

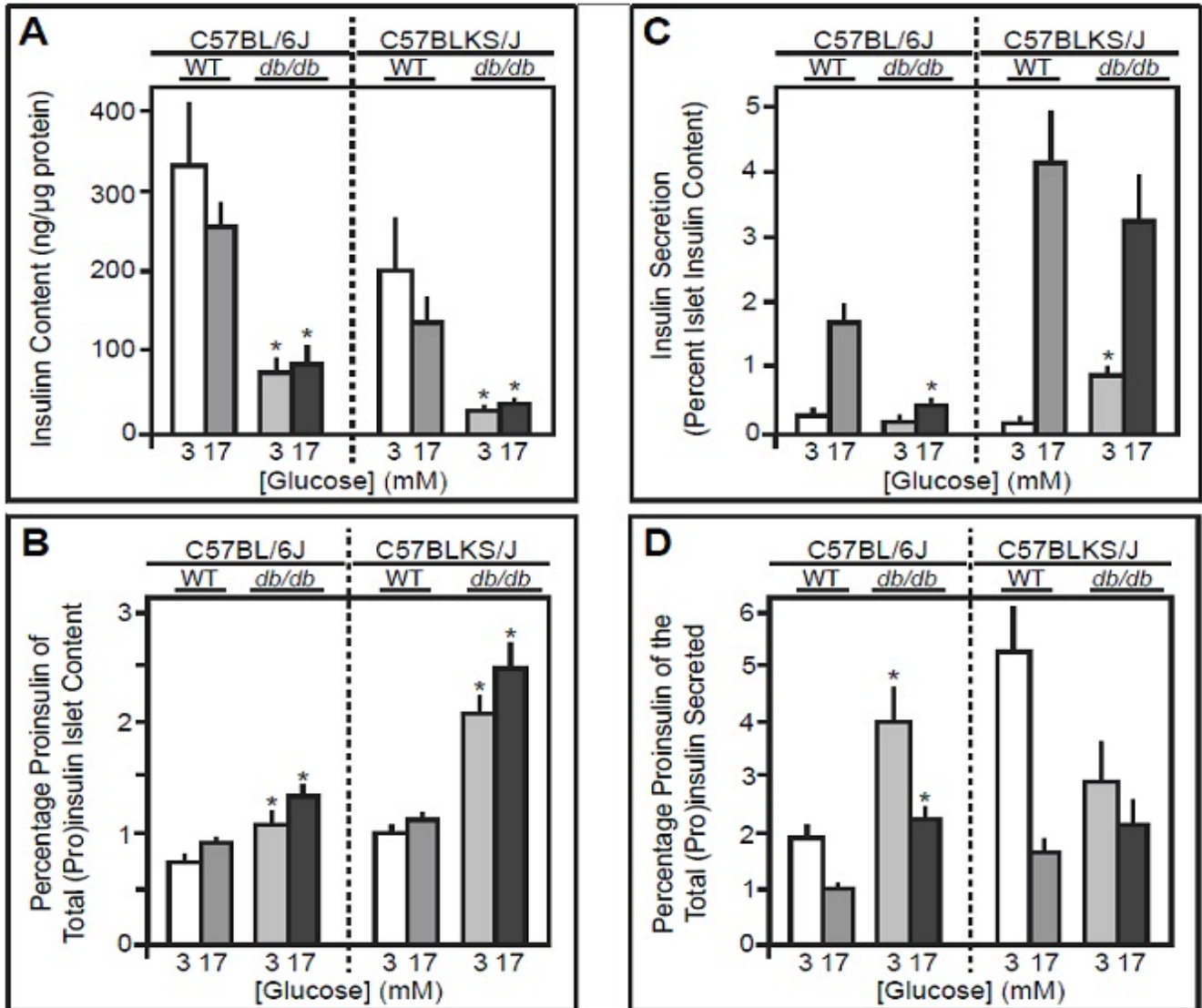


C57BLKS/J *db/db*



SUPPLEMENTARY DATA

Supplementary Figure S5. Insulin content, secretion and proinsulin:insulin ratio in freshly isolated islets. Isolated islets from control (WT) and *db/db* mice were treated with glucose (3 mM or 17 mM for 3.5 h), and then proinsulin and insulin concentrations measured in the islet lysates and the incubation media by ELISA. **(A)** Islet insulin content normalized to islet protein content. **(B)** Islet proinsulin percentage of the total insulin+proinsulin content. **(C)** Secreted insulin normalized to islet insulin content. **(D)** Percentage of proinsulin of the total insulin+proinsulin secreted. Results are presented as mean \pm SE ($n \geq 5$), where * indicates a statistically significant difference of $p \leq 0.05$ vs. respective (WT) controls.



SUPPLEMENTARY DATA

Supplementary Figure S6. Insulin content and proinsulin:insulin ratio in overnight-recovered islets. Isolated islets from control (WT) and *db/db* mice were cultured overnight in RPMI medium containing normoglycemic 5.6 mM glucose prior to treatment with basal 3 mM or stimulatory 17 mM glucose for 3.5 hours. Proinsulin and insulin concentrations were then measured in the islet lysates and incubation media by ELISA. **(A)** Islet insulin content normalized to islet protein content. **(B)** Islet proinsulin percentage of the total insulin+proinsulin content. **(C)** Secreted insulin normalized to islet insulin content. **(D)** Percentage of proinsulin of the total insulin+proinsulin secreted. Results are presented as mean \pm SE ($n \geq 5$), where * indicates a statistically significant difference of $p \leq 0.05$ vs. respective (WT) controls.

